Published in final edited form as:
Neurosurgery. 2009 September ; 65(3): 579–586. doi:10.1227/01.NEU.0000350229.77462.2F.

Anatomical compression due to high volume convection-enhanced delivery to the brain

Francisco Valles, B.S.[1], **Massimo S. Fiandaca, M.D.**[1], **John Bringas, B.S.**[1], **Peter Dickinson, B.V.Sc., Ph.D**[2], **Richard LeCouteur, B.V.Sc., Ph.D**[2], **Robert Higgins, D.V.M., Ph.D.**[2], **Mitchel Berger, M.D.**[1], **John Forsayeth, Ph.D.**[1], and **Krystof S. Bankiewicz, M.D., Ph.D.**[1]

[1] Movement Disorder Research Program, Department of Neurological Surgery, University of California, San Francisco, San Francisco, CA 94103

[2] University of California Davis School of Veterinary Medicine, Department of Surgical and Radiological Sciences, Davis, CA 95616

Abstract

Objective—Our group has pioneered the use of gadolinium liposomes (GDL) in convection-enhanced delivery (CED) using real-time MRI (magnetic resonance imaging) to visualize the distribution of therapeutics in in non-human primate (NHP) and canine brain. We have shown that this procedure is highly predictable and safe. In the course of recent studies, however, we noted that infusion of large volumes caused local anatomical alterations, such as ventricular compression, to occur. This study reports our analysis of CED infusions into normal brains and those compromised by tumors and how monitoring the CED infusion with MRI may be helpful in preventing some complications.

Methods—A total of fifty-four CED infusions using gadolinium liposomes (GDL) were performed in seven canines and ten NHPs, and monitored using real-time MRI. The canines, harboring brain tumors, received infusions of GDL as well as a chemotherapeutic agent via CED. The NHPs were normal and received GDL infusions alone. Real-time analysis of the CED infusion was carried looking for proper catheter position, and infusion reflux, leakage, and mass effect. Retrospective analysis allowed assessment of CED volume of distribution versus volume of infusion.

Results—Approximately ten percent of these infusions caused anatomical compression of the ventricles, especially in the canines with tumors. Reflux along the cannula and leakage of infusate into the ventricular CSF or subarachnoid space was seen. Animal behavior, however, did not appear to be affected acutely or during the time course of the study, and no ventricular compression was noted two weeks after the CED infusion on further brain imaging studies.

Conclusion—These findings illustrate the value of being able to monitor infusions with real time MRI in order to identify phenomena such as reflux along the cannula, leakage of infusate, and ventricular compression. Especially in tumor patients, the latter could be associated with morbidity.

Keywords

Convection-enhanced delivery; Real-time imaging; Infusion Gadoteridol; Liposomes; MRI

Corresponding Author: Krystof S. Bankiewicz, MD, PhD, Department of Neurological Surgery, Movement Disorders Research Program, University of California San Francisco, 1855 Folsom Street, MCB 226, San Francisco, CA 94103, krystof.bankiewicz@ucsf.edu, 415-502-3132 office, 415-502-2864 fax.

Disclosure: We have no personal financial or institutional interest in any of the drugs, materials or devices described in the article.

Introduction

A number of experimental clinical protocols for the treatment of neurological disease require prolonged, chronic infusions into parenchyma of significant volumes of potentially therapeutic agents. For example, a recent Phase 2 study of chronically infused glia-derived neurotrophic factor (GDNF) for the treatment of Parkinson's disease involved daily infusion of 150 μl of recombinant GDNF per day into human putamen for approximately 6 months(16). In another study, 0.75 ml per hour of a therapeutic agent was infused through multiple catheters intra-cerebrally into brain tumors for 96 h (15). In this study, subjects were treated with dexamethasone in order to reduce brain swelling caused by infusion of 72 ml of drug (IL13-PE38QQR). Both of these studies were undertaken without any capacity to monitor the dynamic consequences of such infusions, either in terms of tissue distribution of infusate or of anatomical distortions induced by the infusions. In the latter study, a follow-up analysis showed that efficacious targeting of tumor was critically dependent on precise placement of cannulae (22), emphasizing the need for intra-operative monitoring of infusions.

The use of Gadolinium-loaded liposomes (GDL) as tracers has allowed us to monitor intra-parenchymal infusions in real time by performing the procedure in an MRI (21). As a result of this innovation, we have been able to document previously unknown intra-operative phenomena that have significant implications for intra-parenchymal infusions. For example, reflux and leakage is detected in almost 20% of CED infusions in canines and NHP's investigated with real-time MRI (25). In the present report, we document another potentially limiting factor associated with CED in a retrospective study analyzing 54 infusions. In almost 10% of the infusions, the volumes delivered were large enough to cause anatomical ventricular compression. Histological analysis and/or postoperative MRI confirmed that the infusions did not create a void in the brain tissue. The observed anatomical compression seems to be temporary, resolves spontaneously, and is not associated with behavioral symptoms, and not associated with visible trauma to the brain parenchyma.

Materials and Methods

Experimental Subjects

The protocol for the study of non-human primates (NHP) was reviewed and approved by the Institutional Animal Care and Use Committees at the University of California San Francisco. Adult male Cynomolgus monkeys (*Macaca fascicularis*, n=10, 3-10 kg) were individually housed in stainless steel cages in rooms maintained on a 12-hour light/dark cycle at 18 - 29° C.

Canine pets (n=7, 6-34 kg, 6-11 years), presenting clinically with brain tumors, received liposomal infusions. Experimental protocols were reviewed and approved by the Institutional Animal Care and Use Committee (IACUC) at the University of California Davis and the VMTH Clinical Trials Review Board (CTRB). All animals had a complete physical and neurological examination prior to the procedure and were evaluated at various stages of the study.

Liposome preparation

Liposomes containing the MRI contrast agent, Gadoteridol (Prohance; Bracco Diagnostics, Princeton, NJ), were synthesized as previously described (21). Gadoteridol-loaded liposomes (GDL) of mean diameter 124 ± 24.4 nm were suspended in HEPES-buffered saline (5 mM HEPES, 135 mM NaCl, pH 6.5).

Quantitation of liposome-entrapped Gadoteridol by MRI

The concentration of Gadoteridol entrapped in the liposomes was determined from nuclear MR relaxivity measurements. The relationship between the change in the intrinsic relaxation rate imposed by a paramagnetic agent (ΔR), also known as "T1 shortening," and the concentration of the agent is defined by the equation: $\Delta R = r_1[\text{agent}]$, in which r_1 = relaxivity of the paramagnetic agent and $\Delta R = (1/T1_{observed} - 1/T1_{intrinsic})$. As Gadoteridol was encapsulated within the liposome, we corrected for the change in the observed T1 imposed by the lipid by measurement of the T1 of solubilized liposomes, with and without Gadoteridol, by means of an iterative inversion-recovery *MRI* sequence on a 2-Tesla Brucker Omega scanner (Brucker Medical, Karlsruhe, Germany). The relaxivity of Gadoteridol had been empirically derived previously on the same system and had a value of 4.07 $mM^{-1}sec^{-1}$. The concentration of the encapsulated Gadoteridol was then calculated with the following equation: $[\text{Gadoteridol}] = [(1/T1_{wGado}) - (1/T1_{w/oGado})]/4.07$.

Liposome Infusion in NHP

NHP received a baseline MRI scan, and underwent neurosurgical procedures to position an MRI-compatible guide-cannula within specific regions of the brain (e.g. putamen and corona radiata). Infusions were performed according to previously established CED techniques for NHP (3). Each guide-cannula was specifically customized for the procedure and stereotactically guided to reach its target with coordinates generated by MRI. An initial infusion rate of 0.1 μl/min was applied and increased at 10-min intervals to 0.2, 0.5, 0.8, 1.0 μl/min, up to 5 μl/min. Vital signs, such as heart rate and pO_2, were monitored throughout the procedure. Ten minutes after the completion of the infusion the cannulae were raised out of the brain parenchyma at a rate of 1 mm/min until completely out. Each animal received infusion volumes (Vi) between 700 μl and 40 μl of liposomal Gadoteridol (GDL) at each target site. Infusion intervals varied based on the volume delivered and target, from 240 to 50 minutes. The GDL injected corresponded to a formulated concentration of 10 mM phospholipids and 5 mM Gadoteridol. Each animal received up to three infusions per trial, with a rest period of 4 weeks between trials.

Liposome Infusion in Canines

Animals received a baseline MRI, and infusions were performed according to the previously established CED techniques for canines (8). Briefly, each cannula was stereotactically guided to the brain target. All guide cannulae were left in place for the duration of the study to allow repeated infusions. The dogs were placed in the MRI scanner; the infusion cannulae were inserted into the brain parenchyma through the guide cannula and secured following attachment of drug-loading and infusion lines. The infusion rates were typically 0.1, 0.2, 0.5, 0.8, 1.0, 1.5, 2.0, 2.5, 3.0 μl/min, increasing at 10-min intervals. Several infusions exceeded these rates, delivering larger volumes. Infused volumes (Vi) in our canine patients varied according to the location and size of the tumor, from 2100 μl over 230 minutes to 70 μl over 60 minutes. Intra-tumoral sites were infused with GDL (1.85-3.7mM Gd) and the chemotherapeutic agent Irinotecan (CPT-11; 48.2 mg/ml). Non-tumor sites (thalamus, putamen) were infused with liposomes containing Gadoteridol alone. Infusions were repeated approximately 4 to 8 weeks after the initial infusion. Animals were re-infused with gadolinium-loaded liposomes or gadolinium/CPT-11-loaded liposomes.

MRI Acquisition

T1-weighted images of the primates' brains were acquired on a 1.5 Tesla Signa LX scanner (GE Medical Systems, Waukesha, WI) with a 5″ surface coil on the animal's head, parallel to the floor. Prior to insertion of the infusion catheters, baseline spoiled gradient echo (SPGR) images were taken: repetition time (TR)/echo time (TE)/flip angle = 28 ms/8 ms/40°, number

of excitations (NEX) = 4, matrix = 256 × 192, field of view (FOV) = 16 cm × 12 cm, slice thickness = 1 mm. These parameters resulted in a 0.391 mm^3 voxel volume. Once the catheters were inserted and the infusion started, SPGR scans were taken continuously throughout the infusion. The scan-time was dependent on the number of slices needed to cover the extent of the infusion and ranged from 10 - 12 min.

Infusion Volume and Ventricular Cross Section Area Quantification from MR Images

The volume of liposomal distribution within each infused brain region was quantified on an Apple Macintosh G4 computer with OsiriX® Medical Imaging Software (v.3.0.1). The OsiriX software reads all data specifications from the MR images. The coronal MRI image with the largest infusion cross-sectional area was selected. A time-course of the cross-sectional area of the ventricle during the infusion and a time-course of the infusion volume of distribution (Vd) were both measured with OsiriX's region of interest (ROI) tool. Cross-sectional area was normalized to 100% at the beginning of the infusion. Percentage of ventricle cross-section was plotted against the infusion volume. Seven non-human primates underwent 29 infusions, and 10 canines underwent 25 infusions, for a total of 54 distinct infusions.

Histology

All NHP brain sections were stained with Hematoxylin and Eosin for gross and microscopic assessment of pathology around cannula tract.

Results

Convection of GDL allows us to monitor the progress of CED *in vivo*, in real time, via MR imaging, referred to as real-time convective delivery (RCD). We used this imaging modality to track the distribution of therapeutics in various regions of canine and non-human primate brains. Five (9.3%) of the 54 infusions resulted in noticeable compression of the ventricles. Fig. 1 shows the compression observed in the right ventricle during an intra-tumoral RCD for a naturally occurring tumor in a canine. A midline shift and tumor-associated mass effect were present prior to infusion. We observed increasing mass effect during the RCD with compression of the ventricular system.

The ventricular compression observed was more clearly seen in canines with brain tumors compared to NHPs (none of which harbored tumors). Fig. 2 shows typical anatomical compression with RCD in NHP versus canine. Although the NHP brain tolerates the infusion volume (Vi) without significant mass effect or ventricular compression, the same cannot be said for the canine brain tumor patients. Canine ventricular compression was readily visible in part due to their larger ventricles relative to size of the parenchyma. The anatomical compression that occurs in both NHP and canine subjects during the infusion spontaneously resolves at some point (the time course is yet to be determined) after RCD, with the ventricles returning to normal size within two weeks (Fig. 2C, 2F). Fig. 2F shows that the right ventricle expanded to a size larger than in the pre-infusion MRI (Fig. 2D), suggesting a therapeutic effect of CPT-11 RCD on the tumor, with reduction of tumor size and local mass effect compared to the pre-infusion MRI (compare Fig. 2D with 2F).

Figure 3 shows the relationship between the volume of distribution (Vd) vs. percentage ventricular area compression for the five ventricular compression cases. Ventricular cross-sectional area declines more rapidly in the canine subjects than in NHPs for a given Vd. Complete right ventricular compression occurs in the canines at an infusion volume of 407 ± 59 μl (Fig. 3), whereas in the NHPs complete compression is reached at 672 ± 52 μl.

The average distribution volume that caused detectable (20%) compression and complete ventricular compression was compared in Fig. 4. Canines show a much lower threshold for visible anatomical compression (186 ± 17 μl) when compared to non-human primates (352 ± 77 μl). Complete ventricular compression occurred at an infused volume almost 300 μl lower in canines than in monkeys. Complete ventricular compression may occur in canines much earlier, due possibly to the relative sizes of the canine and primate brains. Since the primate brains are larger, they require a larger volume of infusate to show a significant mass effect. Alternatively, the mass effect in canines might be more readily observed due to the non-compressible, less porous nature of the tumor parenchyma exacerbating the mass effect of the liposomal infusion.

The large infusion volumes achieved could have caused a parenchymal tear in our subjects. Figure 5 shows both the T1 MR image and the T2 MR image of a NHP infusion. The T1 MRI shows the distribution of the infusion, while the T2 MRI shows that the parenchyma was not compromised, since there is no hyperintensity noted in the parenchyma at the site of infusion (hypointense tip of cannula). The mass effect observed in ventricular compression cases is, therefore, likely due to the liposomal infusion distributing throughout the extracellular space (ECS), rather than forming a liquid pocket with parenchymal disruption, that in turn caused anatomical displacement.

To demonstrate further that no parenchymal tear occurred as a result of the RCD, the histology slide for this monkey was analyzed. Figure 6 shows an H&E stain of the monkey in Fig. 5. The histology indicates that no parenchymal tear occurred near the infusion site (indicated by arrow, Fig. 6 A). Moreover, no parenchymal tear is visible around the cannula tip (Fig. 6 B and C), suggesting that the infusion percolated through the ECS and did not form a liquid pocket causing anatomical displacement. The distal cannula track is not visible in this histologic section due to the cannula path moving out of the plane of the tissue section, the small diameter of the distal infusion catheter, and the minimal associated tissue reaction (see Fig. 6 B and C).

Discussion

Operative neurosurgery has recently entered an exciting era of guided surgery or neuro-navigation. Application of this novel technology is beginning to have a significant impact in a variety of intracranial procedures (28). Neurosurgery is using intra-operative MRI regularly in areas of neuro-oncology (10,33,34) and functional neurosurgery (2,20,30). Intra-operative MRI provides real-time visualization, appreciation for anatomical changes during surgery, and improved precision in guiding surgical interventions, thereby increasing surgical safety (28).

Multiple clinical trials are starting to use CED as a means of delivery for intra-cerebral malignancies (11,15,22,29), as well as for neurodegenerative disorders like Parkinson's disease (9,19,23). Accurate cannula positioning (22), correct cannula design (14), optimal cannula size, infusate concentration, and tissue sealing time around the cannula are critical for a successful CED procedure (7). Unfortunately, mixed results of clinical trials have been reported in the absence of real-time visual guidance (13,15,18). It remains unclear as to whether the variability in these results are related to lack of efficacy of the therapeutic, variability in response of patients to the therapeutic, lack of consistent volumetric delivery of the therapeutic to the target, or some additional factor(s) yet to be defined. We postulate that testing of therapeutics in the brain via CED may require a greater precision in targeting, direct visualization of therapeutic volume of distribution, and real-time scrutiny of the CED process for complicating factors (e.g. reflux, leakage, and delivery beyond the intended volume). At this point, RCD is one of the few methods accurate enough to provide us with all of this information. Our group has recently investigated the pattern of distribution of gadolinium (Gd)-DTPA and Gd-liposomes (GDL) convected into brain parenchyma of NHPs (unpublished data). This study was intended to show

whether there were differences in their distribution using our CED protocols. We have noted co-distribution of these two tracers and lack of significant differences between them in the NHP brain.

Our data suggest that large CED infusion volumes, especially over a short period of time, can cause anatomical shifting, especially in brains with compromised physiology due to tumor (as in our canine patients). Bruce and colleagues (6) saw similar findings in a rat glioma model treated with a “clysis” procedure. They found increased intracranial pressure (ICP) in tumor-bearing animals as a baseline and a greater tendency for decompensation in animals with significant mass effect and elevated ICP following infusion of larger volumes over shorter intervals, as opposed to animals not harboring significant tumors. Although the NHP's in our study did not have intracranial mass lesions, and probably had normal intracranial volume/pressure compensatory mechanisms, even in these animals the safeguards could eventually be overcome with higher infused volumes and flow rates, causing anatomical. The canine patients with tumors appeared much more susceptible to brain shifts associated with CED.

Rapid compensatory physiologic mechanisms in the brain to control ICP in response to mass lesions include shifting of cerebrospinal fluid (CSF) out of the intracranial space and into the spinal compartment, and compression of cerebral veins and venous sinuses (thereby reducing total cerebral blood volume). Once these compensatory mechanisms have been maximally employed, further increase in intracranial volume rapidly increases ICP. Langfitt and colleagues (17) developed this volume-pressure relationship concept in NHP's by evaluating ICP in response to gradual increases in volume of an intracranial balloon. The compensatory mechanisms mentioned above are in effect during the high compliance phase, where the ICP remains normal. As the volume increases and compensatory mechanisms are exhausted, the low compliance phase is entered during which ICP elevates to critical levels.

In principle, two mechanisms can be considered in the process by which mass is transported in the interstitial space, namely, bulk fluid movement under the action of hydrostatic pressure gradient (convection), and molecular transport under the action of a concentration gradient (diffusion) (12). Whereas CED relies mainly on convection to deliver therapeutics, there is some diffusion at the periphery of the CED infusion. Barriers to diffusion or convection affect distribution of infusate.

Tumor parenchyma effects on convection are the primary forces influencing the infusion distribution. To discern the effects on convection, interstitial fluid velocities need to be measured. Since measuring interstitial fluid velocities *in vivo* is difficult, several researchers have developed mathematical models based on physical principles to predict fluid transport that occurs during CED. Predictions from these models suggest that the tumor core has an elevated interstitial fluid pressure (4), and that tumors have an outward flow of extracellular fluid at the tumor periphery (24). These two processes lead to experimentally verifiable, radially outward convection that opposes the inward diffusion (or inward convection) (4). This pressurized outward flow from the nuclear core of the tumor creates an environment that a CED infusion has to overcome to perfuse a tumor, unless the catheter is within the lesion. Although direct CED infusion into experimental tumors has shown high concentrations achieved within the lesion, the increased interstitial pressure in these lesions also increases the clearance rate of the therapeutic out of the tumor (27). In many cases, therefore, despite excellent coverage of the tumor via CED, the therapeutic may become less effective or ineffective due to it's rapid clearance (reduced concentration-time product) by the outward flow of the intratumoral extracellular fluid (1). Future strategies will need to include options for altering these interstitial fluid dynamics to enhance the effectiveness of therapeutics delivered by CED.

Tumor barriers to diffusion play a role in the CED perfusion of tumor parenchyma. Among the phenotypic characteristics associated with malignant glioblastoma multiforme are rapid growth, high glucose consumption, intra-tumoral necrosis, hypoxia, and vasogenic brain edema (5). Greater edema should allow greater diffusion due to larger ECS; however, diffusion is impeded in tumors. A diffusion barrier found is the tumor extracellular matrix composition. Tumor malignancy grade strongly corresponds to an increase in ECS volume, accompanied by a change in ECS structure manifested by an increase in diffusion barriers for small molecules (26). In contrast to low-grade tumors, where the diffusion of molecules is reduced mainly by the presence of a dense network of tumor cell processes, the increase of ECS barriers in high-grade gliomas is caused by the overproduction of certain components of the extracellular matrix (ECM), mainly tenascin (31,32). ECM glycoproteins not only stabilize the ECS volume, but also serve as a substrate for adhesion and subsequent migration of the tumor cells through the enlarged ECS. These same alterations in ECS structure may hinder the diffusion of neuroactive substances or even molecules of drugs into the neoplastic tissue (31). These barriers in diffusion caused by tumor parenchyma create a less permeable medium through which a CED infusion has to infiltrate.

The barriers to therapeutic convection and therapeutic diffusion in tumor parenchyma create obstacles that CED infusions have to overcome to perfuse a tumor. We surmise that these barriers cause CED infusions to partly displace the tumor tissue in an attempt to perfuse it. This tumor displacement causes enhanced mass effects during CED infusions leading to increased ventricular compressions observed. This information is especially important to understand and corroborate since CED is being used in human clinical trials for brain tumors, some of which suffer altered physiology and compensatory mechanisms.

Conclusions

This study illustrates the utility of MRI-monitored CED infusions with respect to intra-operative dynamic changes in brain anatomy as a consequence of voluminous infusions of therapeutic agents into brain parenchyma. CED infusions are a complex delivery system that should rely on intra-operative MR imaging to discern any potential adverse effects of the therapy such as leakage (25) or mass effects described here.

Acknowledgments

This work was supported by NIH Grants, NS050156-01A2 (NINDS), P50 CA097257 (SPORE) and 1 P01 CA118816-02 (NCI). We also thank Robert Thorne (NYU Medical School) for helpful discussions.

References

1. Ali MJ, Navlitloha Y, Vavra MW, Kang EWY, Itskovitch AC, Molnar P, Levy RM, Groothuis DR. Isolation of drug delivery from drug effect: Problems of optimizing drug delivery parameters. Neuro-Oncology 2006;8:109–118. [PubMed: 16533759]
2. Archip N, Clatz O, Whalen S, Kacher D, Federov D, Kot A, Chrisochoides N, Jolesz F, Golby A, Black PM, Warfield SK. Non-rigid alignment of pre-operative MRI, fMRI, and DT-MRI with intra-operative MRI for enhanced visualization and navigation in image-guided neurosurgery. Neuroimage 2007;35:609–624. [PubMed: 17289403]
3. Bankiewicz KS, Eberling JL, Kohutnicka M, Jagust W, Pivirotto P, Bringas J, Cunningham J, Budinger TF, Harvey-White J. Convection-enhanced delivery of AAV vector in parkinsonian monkeys; in vivo detection of gene expression and restoration of dopaminergic function using pro-drug approach. Exp Neurol 2000;164:2–14. [PubMed: 10877910]
4. Baxter LT, Jain RK. Transport of fluid and macromolecules in tumors. I. Role of interstitial pressure and convection. Microvasc Res 1989;37:77–104. [PubMed: 2646512]

5. Behin A, Hoang-Xuan K, Carpentier AF, Delattre JY. Primary brain tumours in adults. Lancet 2003;361:323–331. [PubMed: 12559880]
6. Bruce JN, Falavigna A, Johnson JP, Hall JS, Birch BD, Yoon JT, Wu EX, Fine RL, Parsa AT. Intracerebral clysis in a rat glioma model. Neurosurgery 2000;46:683–691. [PubMed: 10719865]
7. Chen MY, Lonser RR, Morrison PF, Governale LS, Oldfield EH. Variables affecting convection-enhanced delivery to the striatum: a systematic examination of rate of infusion, cannula size, infusate concentration, and tissue-cannula sealing time. J Neurosurg 1999;90:315–320. [PubMed: 9950503]
8. Dickinson PJ, LeCouteur RA, Higgins RJ, Bringas JR, Roberts B, Larson RF, Yamashita Y, Krauze M, Noble CO, Drummond D, Kirpotin DB, Park JW, Berger MS, Bankiewicz KS. Canine model of convection-enhanced delivery of liposomes containing CPT-11 monitored with real-time magnetic resonance imaging: laboratory investigation. J Neurosurg 2008;108:989–998. [PubMed: 18447717]
9. Eberling JL, Jagust WJ, Christine CW, Starr P, Larson P, Bankiewicz KS, Aminoff MJ. Results from a phase I safety trial of hAADC gene therapy for Parkinson disease. Neurology 2008;70:1980–1983. [PubMed: 18401019]
10. Hata N, Muragaki Y, Inomata T, Maruyama T, Iseki H, Hori T, Dohi T. Intraoperative tumor segmentation and volume measurement in MRI-guided glioma surgery for tumor resection rate control. Acad Radiol 2005;12:116–122. [PubMed: 15691732]
11. Husain SR, Puri RK. Interleukin-13 receptor-directed cytotoxin for malignant glioma therapy: from bench to bedside. J Neurooncology 2003;65:37–48.
12. Kim D, Armenante PM, Duran WN. Mathematical modeling of mass transfer in microvascular wall and interstitial space. Microvasc Res 1990;40:358–378. [PubMed: 2084501]
13. Kordower JH, Palfi S, Chen EY, Ma SY, Sendera T, Cochran EJ, Mufson EJ, Penn R, Goetz CG, Comella CD. Clinicopathological findings following intraventricular glial-derived neurotrophic factor treatment in a patient with Parkinson's disease. Ann Neurol 1999;46:419–424. [PubMed: 10482276]
14. Krauze MT, Saito R, Noble C, Tamas M, Bringas J, Park JW, Berger MS, Bankiewicz K. Reflux-free cannula for convection-enhanced high-speed delivery of therapeutic agents. J Neurosurg 2005;103:923–929. [PubMed: 16304999]
15. Kunwar S, Prados MD, Chang SM, Berger MS, Lang FF, Piepmeier JM, Sampson JH, Ram Z, Gutin PH, Gibbons RD, Aldape KD, Croteau DJ, Sherman JW, Puri RK. Direct intracerebral delivery of cintredekin besudotox (IL13-PE38QQR) in recurrent malignant glioma: a report by the Cintredekin Besudotox Intraparenchymal Study Group. J Clin Oncol 2007;25:837–844. [PubMed: 17327604]
16. Lang AE, Gill S, Patel NK, Lozano A, Nutt JG, Penn R, Brooks DJ, Hotton G, Moro E, Heywood P, Brodsky MA, Burchiel K, Kelly P, Dalvi A, Scott B, Stacy M, Turner D, Wooten VG, Elias WJ, Laws ER, Dhawan V, Stoessl AJ, Matcham J, Coffey RJ, Traub M. Randomized controlled trial of intraputamenal glial cell line-derived neurotrophic factor infusion in Parkinson disease. Ann Neurol 2006;59:459–466. [PubMed: 16429411]
17. Langfitt TW, Weinstein JD, Kassell NF. Cerebral vasomotor paralysis produced by intracranial hypertension. Neurology 1965;15:622–641. [PubMed: 14306322]
18. Levy RM, Major E, Ali MJ, Cohen B, Groothius D. Convection-enhanced intraparenchymal delivery (CEID) of cytosine arabinoside (AraC) for the treatment of HIV-related progressive multifocal leukoencephalopathy (PML). J Neurovirol 2001;7:382–385. [PubMed: 11517421]
19. Morrison PF, Lonser RR, Oldfield EH. Convective delivery of glial cell line-derived neurotrophic factor in the human putamen. J Neurosurg 2007;107:74–83. [PubMed: 17639877]
20. Rasmussen IA Jr, Lindseth F, Rygh OM, Berntsen EM, Selbekk T, Xu J, Nagelhus Hernes TA, Harg E, Haberg A, Unsgaard G. Functional neuronavigation combined with intra-operative 3D ultrasound: initial experiences during surgical resections close to eloquent brain areas and future directions in automatic brain shift compensation of preoperative data. Acta Neurochir (Wien) 2007;149:365–378. [PubMed: 17308976]
21. Saito R, Krauze MT, Bringas JR, Noble C, McKnight TR, Jackson P, Wendland MF, Mamot C, Drummond DC, Kirpotin DB, Hong K, Berger MS, Park JW, Bankiewicz KS. Gadolinium-loaded liposomes allow for real-time magnetic resonance imaging of convection-enhanced delivery in the primate brain. Exp Neurol 2005;196:381–389. [PubMed: 16197944]

22. Sampson JH, Brady ML, Petry NA, Croteau D, Friedman AH, Friedman HS, Wong T, Bigner DD, Pastan I, Puri RK, Pedain C. Intracerebral infusate distribution by convection-enhanced delivery in humans with malignant gliomas: descriptive effects of target anatomy and catheter positioning. Neurosurgery 2007;60:89–98.ONS
23. Slevin JT, Gash DM, Smith CD, Gerhardt GA, Kryscio R, Chebrolu H, Walton A, Wagner R, Young AB. Unilateral intraputamenal glial cell line-derived neurotrophic factor in patients with Parkinson disease: response to 1 year of treatment and 1 year of withdrawal. J Neurosurg 2007;106:614–620. [PubMed: 17432712]
24. Smith JH, Humphrey JA. Interstitial transport and transvascular fluid exchange during infusion into brain and tumor tissue. Microvasc Res 2007;73:58–73. [PubMed: 17069863]
25. Varenika V, Dickenson P, Bringas J, LeCouteur R, Higgins R, Park JW, Fiandaca M, Berger MS, Sampson JH, Bankiewicz KS. Real-time imaging of CED in the brain permits detection of infusate leakage. J Neurosurg 2008;109:874–880. [PubMed: 18976077]
26. Vargova L, Homola A, Zamecnik J, Tichy M, Benes V, Sykova E. Diffusion parameters of the extracellular space in human gliomas. Glia 2003;42:77–88. [PubMed: 12594739]
27. Vavra M, Ali MJ, Kang EWY, Navlitloha Y, Ebert A, Allen CV, Groothuis DR. Comparative pharmacokinetics of 14-C-sucrose in RG-2 rat gliomas after intravenous and convection-enhanced delivery. Neuro-Oncology 2004;6:104–112. [PubMed: 15134624]
28. Wadley J, Kitchen N, Thomas D. Image-guided neurosurgery. Hosp Med 1999;60:34–38. [PubMed: 10197096]
29. Weber FW, Floeth F, Asher A, Bucholz R, Berger M, Prados M, Chang S, Bruce J, Hall W, Rainov NG, Westphal M, Warnick RE, Rand RW, Rommell F, Pan H, Hingorani VN, Puri RK. Local convection enhanced delivery of IL4-Pseudomonas exotoxin (NBI-3001) for treatment of patients with recurrent malignant glioma. Acta Neurochir Suppl 2003;88:93–103. [PubMed: 14531567]
30. Wunderlich AP, Gron G, Braun V. Functional MR imaging of working memory before neurosurgery. Z Med Phys 2007;17:250–257. [PubMed: 18254547]
31. Zamecnik J. The extracellular space and matrix of gliomas. Acta Neuropathol 2005;110:435–442. [PubMed: 16175354]
32. Zamecnik J, Vargova L, Homola A, Kodet R, Sykova E. Extracellular matrix glycoproteins and diffusion barriers in human astrocytic tumours. Neuropathol Appl Neurobiol 2004;30:338–350. [PubMed: 15305979]
33. Zimmermann M, Seifert V, Trantakis C, Kuhnel K, Raabe A, Schneider JP, Dietrich J, Schmidt F. Open MRI-guided microsurgery of intracranial tumours. Preliminary experience using a vertical open MRI-scanner. Acta Neurochir (Wien) 2000;142:177–186. [PubMed: 10795892]
34. Zimmermann M, Seifert V, Trantakis C, Raabe A. Open MRI-guided microsurgery of intracranial tumours in or near eloquent brain areas. Acta Neurochir (Wien) 2001;143:327–337. [PubMed: 11437285]

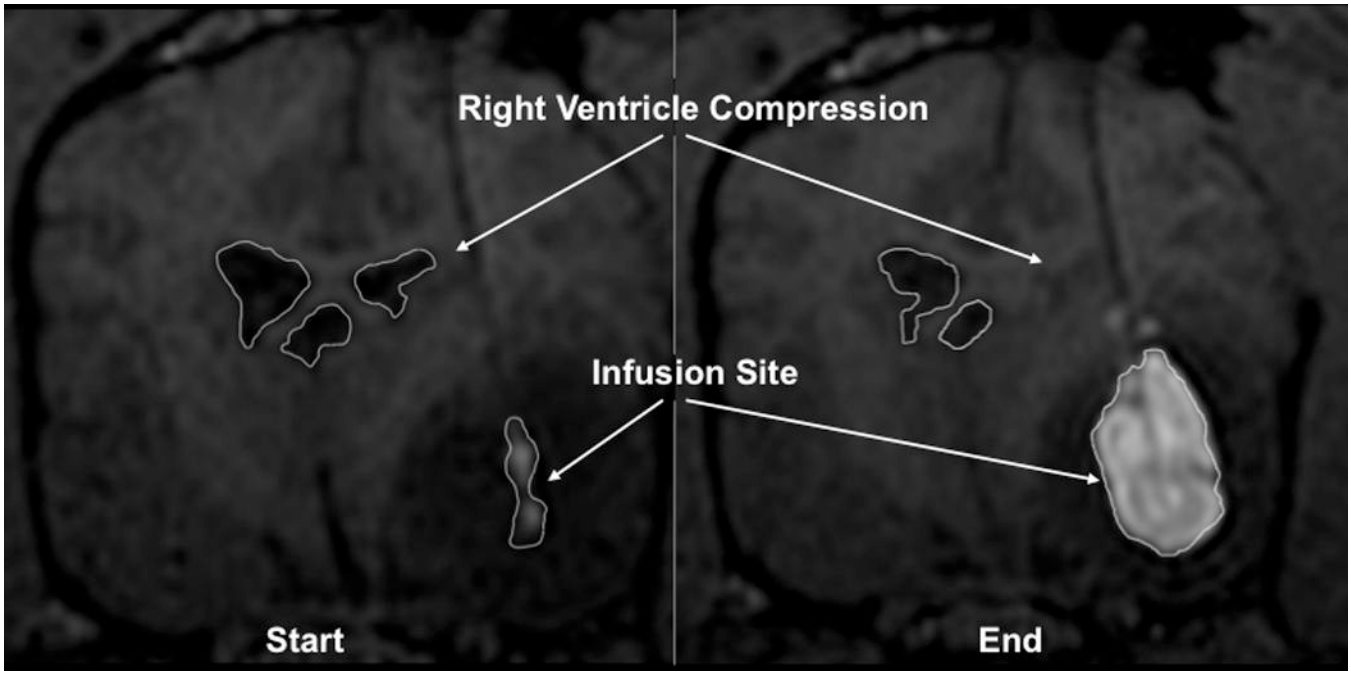

Figure 1. Ventricular compression due to intra-tumoral CED infusion in canine
T1-weighted coronal MRI. Hyperintense area indicates gadolinium/CPT-11 loaded liposomal infusion. The hypointense region surrounding the infusion denotes tumor.

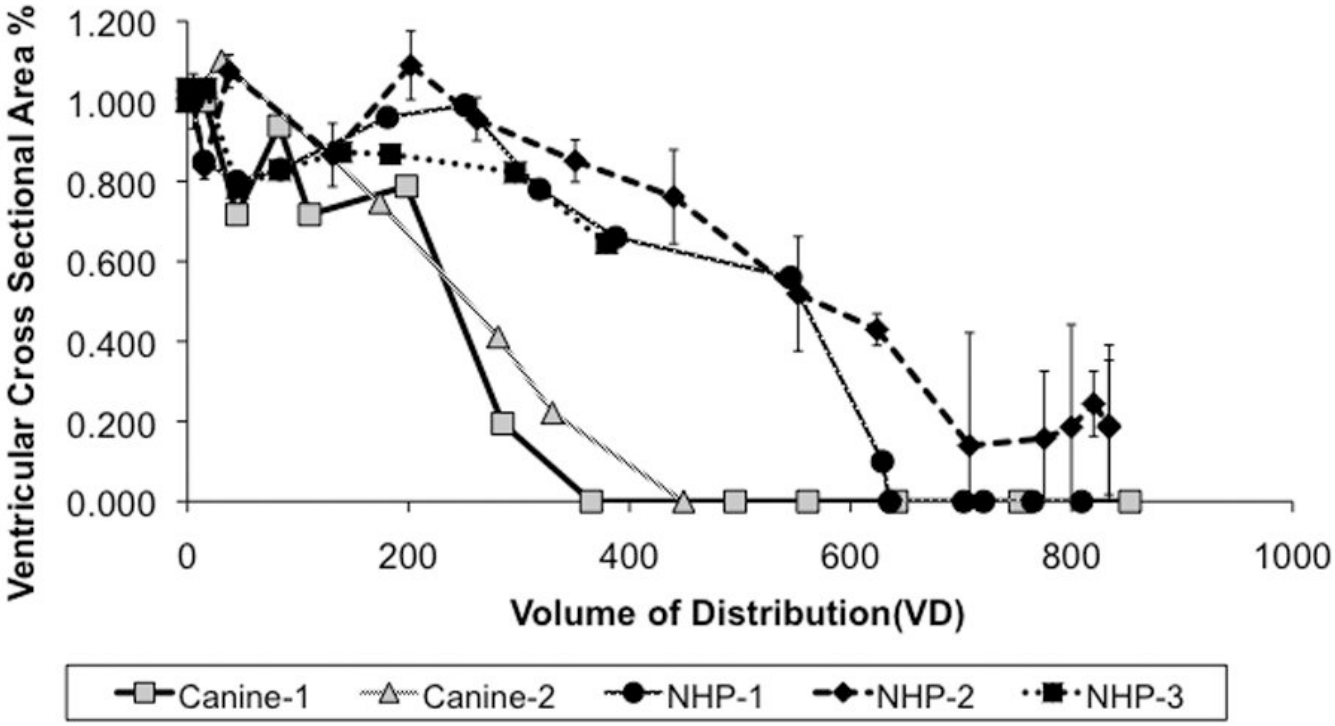

Figure 2. T1-weighted MRIs showing anatomical compression of non-human primate and canine lateral ventricles

The white line drawn outlines the perimeter of the right lateral ventricle on coronal sections. Long white arrows point to the hypointense cannula track. Short white arrows point to the hypointense region of the canine tumor. **A**. MRI of non-human primate (NHP) brain prior to infusion. **B**. NHP brain during infusion. Hyperintense area indicates GDL infusion. **C**. NHP brain 2-weeks after infusion. Outlined right ventricle perimeter indicates ventricle is back to normal size. **D**. MRI of canine brain prior to infusion. **E**. Canine brain during GDL/CPT-11 infusion. Note hyperintense contrast following the hypointense cannula track, suggesting reflux. Outlined right ventricle (white circle) is compressed. **F**. Canine brain 1 month after liposomal infusion. Outlined right ventricle (white circle) is much larger now compared to original study and possibly slightly larger.

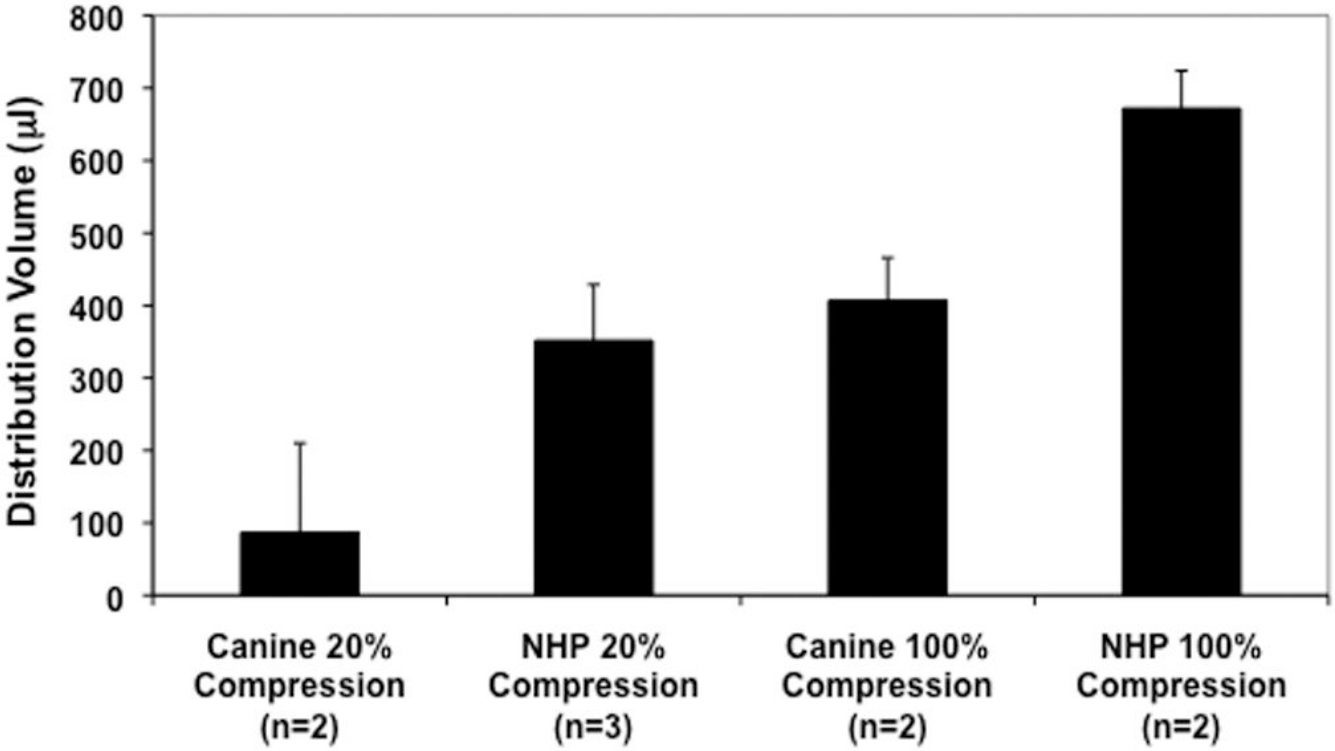

Figure 3. Ventricular compression vs infusion volume

Two canine brain tumor patients and three nonhuman primates showing ventricular compression. The degree of compression as a percentage of the ventricular cross-sectional area is plotted against the volume of distribution of the infusate in the tissue. Both canine patients showed ventricular compression at a much lower volume of distribution than the NHPs.

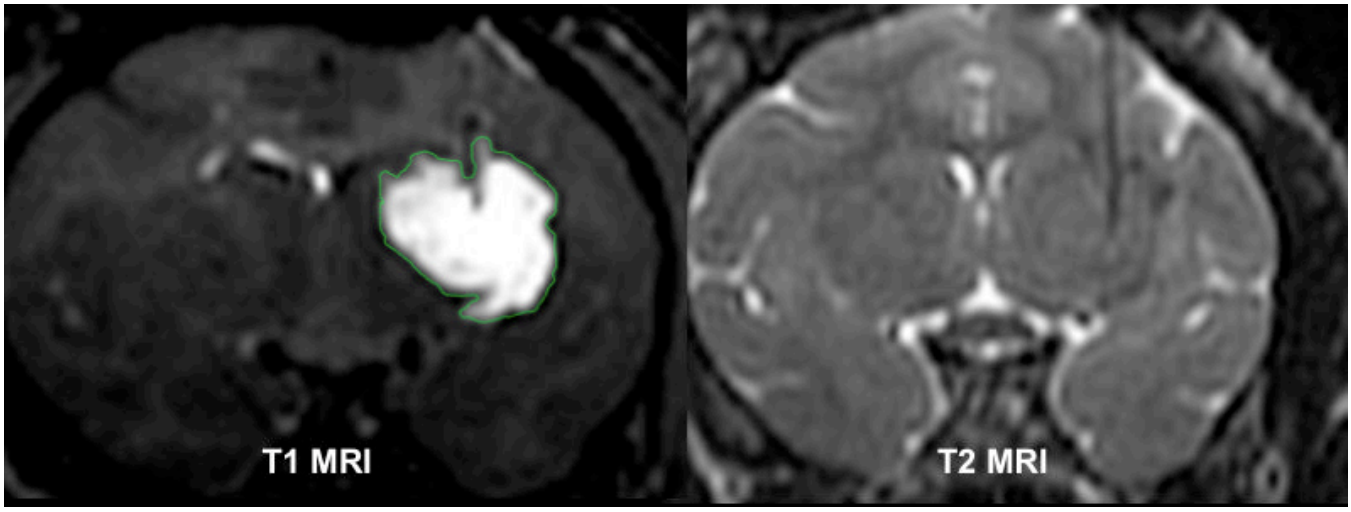

Figure 4. Average infusion volumes for canines and NHP at 20% and 100% ventricular compression

Canine brain tumor patients more readily show ventricular compression at lower volumes of distribution than do NHPs.

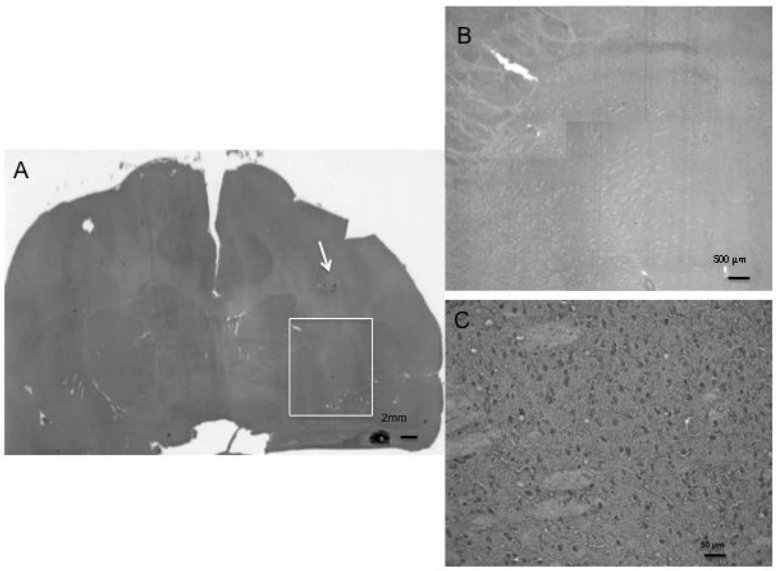

Figure 5. MRI of NHP infusion

Right image shows a T1-weighted image showing extent of GDL infusion. Left image shows a T2-weighted image during the same time point of the infusion. No trauma was detected in the parenchyma except for hypointense line indicative of cannula. Parenchymal trauma or tearing, with collection of fluid at the catheter tip would be expect to show as a region of hyperintensity on T2-weighted images.

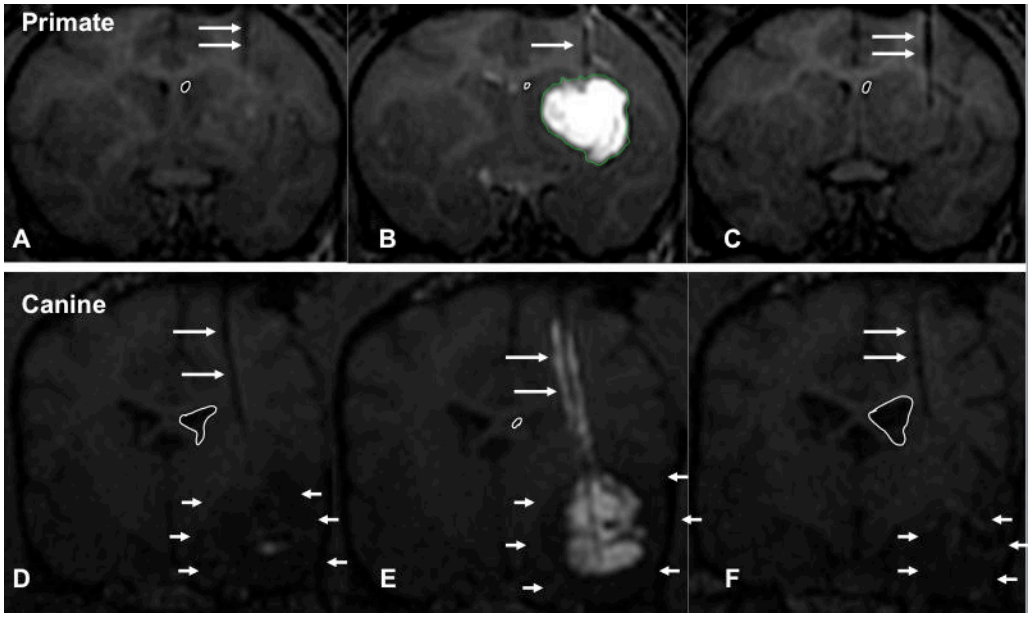

Figure 6. Hematoxylin and eosin stained section of normal non-human primate brain imaged in Figure 5

A. Black and white photo of H&E stain of NHP brain showing the altered parenchyma around the proximal cannula (white arrow). White box depicts the region of the CED infusion noted on Figure 5. Bar is 2 mm in length. B. Low power photomicrograph of region demarcated by white box. This represents the parenchyma infused as seen in the T1-weigthed image of Figure 5. Bar is 500 μm in length. C. Higher power photomicrograph of inset region, showing no inflammatory cellular infiltrate or other evidence of trauma related to the tip of the catheter in this region. The CED infusion perfused the tissue but did not cause a parenchymal tear. Bar is 50 μm in length.